IEEE Photonics Journal
An IEEE Photonics Society Publication

Open Access

High-Peak-Power Acousto-Optically Q-Switched Er:Y_2O_3 Ceramic Laser at $\sim$2.7 μm

Volume 9, Number 4, August 2017

X. J. Ren
Y. Wang
X. L. Fan
J. Zhang
D. Y. Tang
D. Y. Shen

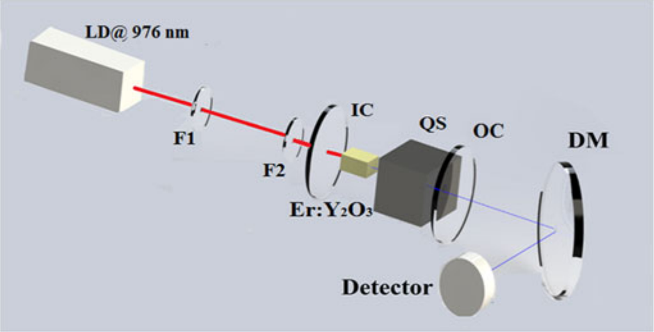

DOI: 10.1109/JPHOT.2017.2716398

High-Peak-Power Acousto-Optically Q-Switched Er:Y_2O_3 Ceramic Laser at ~2.7 μm

X. J. Ren,[1] Y. Wang,[2] X. L. Fan,[1] J. Zhang,[2] D. Y. Tang,[2] and D. Y. Shen[1]

[1]Department of Optical Science and Engineering, Fudan University, Shanghai 200433, China
[2]Jiangsu Key Laboratory of Advanced Laser Materials and Devices, School of Physics and Electronic Engineering, Jiangsu Normal University, Xuzhou 221116, China

DOI:10.1109/JPHOT.2017.2716398

Manuscript received May 4, 2017; revised June 2, 2017; accepted June 13, 2017. Date of publication June 16, 2017; date of current version July 7, 2017. This work was supported by the National Science Foundation of China (NSFC) (61177045, 11274144), NSAF (U1430111), and a project funded by the Priority Academic Development of Jiangsu Higher Education Institutions (PAPD). Corresponding author: D. Y. Shen (e-mail: shendy@fudan.edu.cn).

Abstract: We report on a high-peak-power acousto-optically Q-switched Er:Y_2O_3 ceramic laser operating at room temperature. Stable pulses with a duration of 41–190 ns (FWHM) are generated at approximately 2.7 μm with the repetition rate varying from 0.3 to 10 kHz. The peak power at 0.3-kHz repetition rate is approximately 7.3 kW. An average output power of over 320 mW is generated at a repetition rate of 10 kHz using an output coupler with a transmission of 8%.

Index Terms: Infrared lasers, Q-switched lasers, laser crystals.

1. Introduction

Mid-Infrared lasers operating at ~2.7 μm have found wide application in spectroscopy [1], laser surgery [2], [3], and mid-infrared photonics [4], [5]. The two common approaches to generate lasers at ~2.7 μm are nonlinear frequency conversion and direct generation [6]– [9]. In terms of structural simplicity, the direct-generation approach is preferable. In this approach, the $^4I_{11/2} \rightarrow {}^4I_{13/2}$ transition of Er^{3+} ions is often utilized to directly generate the 2.7-μm laser emission. However, because of the narrow energy gap between the $^4I_{11/2}$ and $^4I_{13/2}$ levels (~3500 cm^{-1}), ions of the $^4I_{11/2}$ manifold are decayed via the multiphonon relaxation process, and the laser oscillation is eventually self-terminated. Thus, to realize 2.7-μm laser oscillations, an optimal amount of doping is required to effectively depopulate the terminal laser level through the well-known concentration-dependent upconversion process $^4I_{13/2} + {}^4I_{13/2} \rightarrow {}^4I_{9/2} + {}^4I_{15/2}$. The optimized doping concentration in conventional YAG is as high as 50 at. % due to the severely nonradiative decay observed in YAG [8], [9]. Unfavorable thermal effects lead to a deterioration in laser operation in such heavily doped laser materials, and thus, the power scaling and high-repetition-rate operation of such laser materials are limited. On the other hand, the optimized doping concentrations decrease to 30 at. %, 15 at. %, and 4 at. %, in YSGG [10]–[12], YLF [13], and CaF_2 [14], respectively, since nonradiative decay is mitigated in hosts with low phonon energy. Pulses of 60 μJ energy and

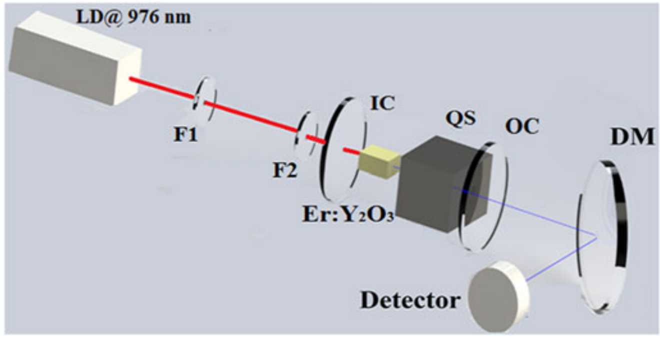

Fig. 1. Schematic of our experimental setup.

$\sim$200 ns duration, and $\sim$0.5 mJ energy and $\sim$77 ns duration have been demonstrated from mechanically Q-switched Er:YLF [13] and electro-optically Q-switched Er:YSGG laser [12]. However, the doping concentrations are still high in YSGG and YLF, while the thermal conductivity of CaF_2 is poor. Thus, the search for laser materials for $\sim$2.7 μm laser operation has assumed research significance.

Cubic sesquioxides have attracted considerable attention due to their superior properties, for e.g., low phonon energy and high thermal conductivity [15], [16]. The optimized doping concentrations of sesquioxides for $\sim$2.7 μm laser oscillation were demonstrated to be $\sim$7 at. % at room temperature (RT) [17], [18] and $\sim$2 at. % at liquid nitrogen temperature [19], [20]. The low doping concentrations result in a significant decrease in the thermal loading density. Moreover, sesquioxides exhibit excellent heat dissipation owing to their high thermal conductivity. In addition, Er-doped sesquioxides have long fluorescence lifetimes, which are beneficial for energy storage [17], [19]. However, it is difficult to grow sesquioxide crystals using the Czochralski method due to their high melting points ($>$2400 °C).

On the other hand, sesquioxide ceramics can be fabricated at temperatures far lower than their melting points. Furthermore, sesquioxide ceramics offer the advantages of rapid and large-scale fabrication, flexibility in producing composite structures, and good thermo-mechanical properties [21]. Very recently, Er^{3+}-doped Lu_2O_3 ceramic was successfully fabricated, with which continuous-wave (CW) lasing at RT was demonstrated with 611 mW of output at $\sim$2.7 μm [22]. Similarly, at liquid nitrogen temperature, efficient lasing at $\sim$2.7 μm was demonstrated from an $Er:Y_2O_3$ ceramic laser, generating over 26 W of CW output power [20]. Passively Q-switched operation of an $Er:Y_2O_3$ ceramic laser using a black-phosphorus saturable absorber generating pulses with a duration of $\sim$4.5 μs and energy of $\sim$0.48 μJ was realized at RT [23].

In this paper, we report on a high-peak-power $\sim$2.7 μm $Er:Y_2O_3$ ceramic laser operating at RT using an acousto-optic (AO) Q-switch (QS). An average output power of over 320 mW is obtained at a pulse repetition frequency (PRF) of 10 kHz in a beam with M^2 values estimated to be about 3.39 and 1.88 along the x- and y-directions, respectively. Stable pulses with a duration of 41-190 ns (FWHM) are generated for repetition rates varying in the range from 0.3 kHz to 10 kHz. A peak power of $\sim$7.3 kW is obtained at a repetition rate of 0.3 kHz. Dual-wavelength operation and red-shift behavior of the output spectrum are observed with increase in pump power. To the best of our knowledge, our laser thus far offers the highest peak power and shortest pulse width among diode-pumped Q-switched lasers in the $\sim$2.7 μm wavelength range.

2. Experimental Setup

The schematic of the Q-switched $Er:Y_2O_3$ ceramic laser is depicted in Fig. 1. In the study, we employed a simple two-mirror resonator with a cavity length of $\sim$75 mm. A flat mirror with high reflectivity (R $>$ 99.8%) at the laser wavelength of $\sim$2.7 μm and high transmission (T $>$ 98%) at the pump wavelength of $\sim$976 nm was used as the input coupler (IC). The plane output coupler (OC)

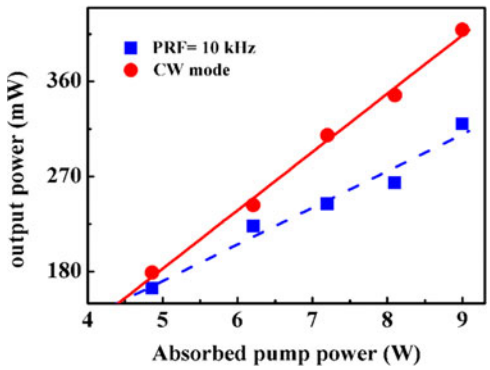

Fig. 2. Continuous-wave (CW) output power and average output power at pulse repetition frequency (PRF) of 10 kHz versus absorbed pump power.

exhibited a transmission of 8% at ~2.7 μm and high transmission at the pump wavelength. The unabsorbed pump light and the laser were separated by a dichroic mirror (DM) with high reflectivity at ~2.7 μm and high transmission at ~976 nm at 45°.

The laser gain medium was a polycrystalline Er:Y_2O_3 ceramic with 7.0 at. % doping concentration. The ceramic was 12 mm in length and 3 $\times$ 2 mm in cross section. Both end facets of the sample were uncoated. The sample was wrapped with indium foil and mounted on a water-cooled copper heat sink maintained at ~10 °C to ensure efficient heat removal. The single-pass absorption efficiency under non-lasing conditions was measured to be about 90% for small signal pumping.

The pump source was a fiber-coupled laser diode (LD) with center wavelength at ~976 nm. The delivery fiber had a core diameter of 105 μm and an output numerical aperture (NA) of less than 0.15. The pump laser was collimated by a plano-convex lens F1 with a focal length of 25 mm and then focused onto the Er:Y_2O_3 sample by a plano-convex lens F2 with a 100-mm focal length. The pump beam diameter inside the Er:Y_2O_3 sample was estimated to be ~420 μm, corresponding to a confocal parameter value of ~26 mm.

A TeO_2 AO (QSG27-2, CETC26) Q-switch was inserted into the resonator and placed several millimeters beyond the ceramic sample. The AO Q-switch had a diffraction efficiency of >55%, an optical transmission of >90%, and an optical rise and fall time of 90 ns (supported by the provider). It was driven with 120 W of radio-frequency power at a frequency of 27.12 MHz and modulated at a tunable switching rate with the use of a function generator (AFG3252, Tektronix).

3. Results

In the CW-operation mode with the AO Q-switch inserted into the cavity, the Er:Y_2O_3 ceramic laser reached threshold at 3.2 W of absorbed pump power. Under 9 W of absorbed pump power, the laser exhibited an output power of 409 mW, corresponding to a slope efficiency of ~5.5% with respect to the absorbed pump power. In the Q-switched operation mode, the laser exhibited an average output power of over 320 mW at a PRF of 10 kHz under 9 W of absorbed pump power, corresponding to a slope efficiency of ~3.5%. We attribute this low efficiency mainly to ceramic sample loss and insertion loss of the AO Q-switch. Fig. 2 shows the CW output power and average output power at 10-kHz PRF as functions of the absorbed pump power. The nearly linear dependences of the output power on the pump power suggest that the laser has promising power-scaling ability.

The pulse characteristics were detected by a fast HgCdTe infrared detector with a rise time of 1.5 ns (PVM-10.6, Vigo System SA) and recorded by a 1-GHz-bandwidth oscilloscope (DSO104A, Keysight). Under 9 W of absorbed pump power, the pulse building time was 2 μs (measured through simultaneous monitoring the radio-frequency signal and the laser pulse) after the Q-switch was turned on at 0.3 kHz. The pulse duration and pulse energy were measured to be 41 ns and 0.3 mJ, respectively, at 0.3 kHz, corresponding to a peak power of ~7.3 kW. When the repetition rate was increased from 0.3 kHz to 10 kHz, the pulse building time increased from 2 μs to 3 μs,

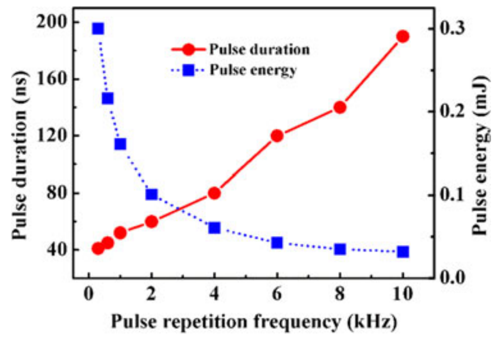

Fig. 3. Pulse duration and pulse energy versus pulse repetition frequency (PRF) under 9 W of absorbed pump power.

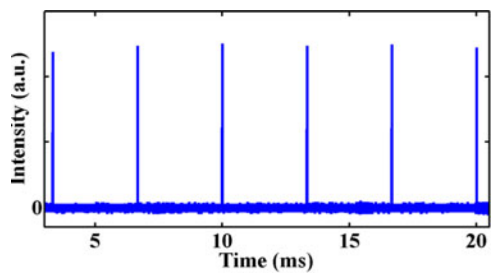

Fig. 4. Typical pulse train at pulse repetition frequency (PRF) of 0.3 kHz.

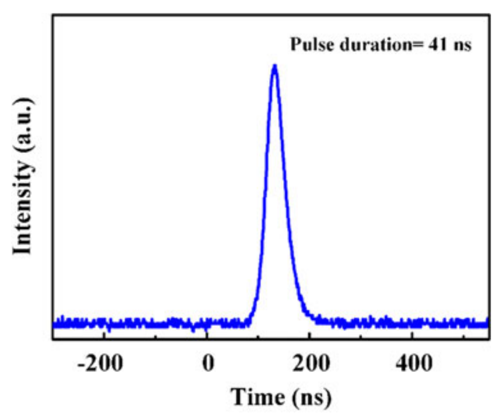

Fig. 5. Single-pulse profile at pulse repetition frequency (PRF) of 0.3 kHz.

the pulse duration increased from 41 ns to 190 ns, and the pulse energy decreased accordingly. The dependencies of the pulse duration and pulse energy on pulse repetition frequency under an absorbed pump power of 9 W are shown in Fig. 3.

The Q-switched pulse trains were observed to be stable at all the repetition rates, and no significant pulse jitter was observed. The typical pulse train and single-pulse profile at 0.3 kHz PRF under 9 W of absorbed pump power are illustrated in Figs. 4 and 5, respectively.

The beam quality at 10 kHz PRF was examined with a beam profiler (NanoScan, Photon Inc., Cambridge, Massachusetts, USA) under 9 W of absorbed pump power. The M^2 factors along the x- and y-directions were estimated to be about 3.39 and 1.88, respectively, by fitting the measured

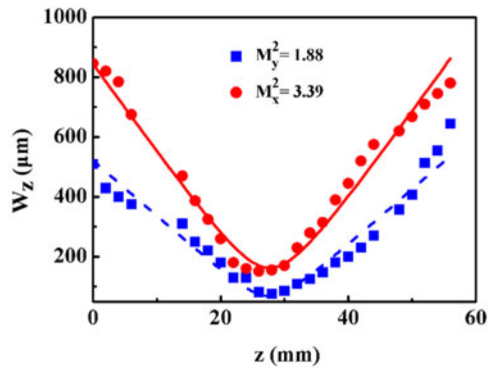

Fig. 6. Beam quality of Er:Y_2O_3 laser.

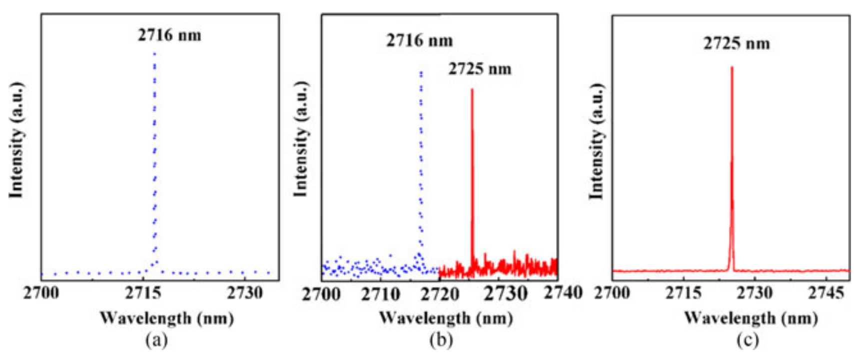

Fig. 7. Spectrum of Er:Y_2O_3 laser.

data with a hyperbolic curve (see Fig. 6). The slight difference of M^2 in the x- and y-directions may be attributed to the asymmetric heat dissipation in the two directions.

The output spectrum of the Er:Y_2O_3 ceramic laser was analyzed with the use of a 0.55-m monochromator with a resolution of 0.2 nm at ~2.7 μm (Omni-λ5005, Zolix). At absorbed pump powers higher than the threshold (3.2 W) and lower than 6.2 W, the emission wavelength centered at 2716 nm [see Fig. 7(a)]. With further increase in pump power, oscillation at a longer wavelength of 2725 nm was observed, and the laser operated simultaneously at 2716 and 2725 nm. The relative intensity of the two wavelengths can be suitably controlled with the pump power level, and further, the two laser signals are highly stable in terms of both amplitude and center-wavelength. Fig. 7(b) shows the output spectrum of the dual-wavelength laser at an absorbed pump power of 7.2 W. When the pump power was increased above 8.1 W, the 2716 nm component disappeared, and only the 2725 nm signal was observed to oscillate [see Fig. 7(c)]. We attribute these spectrum characteristics to the reabsorption of the populated $^4I_{13/2}$ energy level and the fact that the ion populations in both the $^4I_{11/2}$, $^4I_{13/2}$ energy levels and their corresponding Stark sublevels are dependent on the pump power. The dual-wavelength emission may have potential applications in Doppler Lidar and THz-radiation generation.

4. Conclusion

In conclusion, we demonstrated high-peak-power Q-switched operation of an Er:Y_2O_3 ceramic laser at room temperature. Stable pulses with a duration of 41–190 ns were generated at ~2.7 μm with the repetition rate varying from 0.3 to 10 kHz. A peak power of ~7.3 kW was obtained at 0.3 kHz repetition rate, and an average output power of over 320 mW was obtained at 10 kHz repetition rate. Further improvements in laser efficiency should be readily achievable by reducing the resonator loss.

References

[1] N. Cezard *et al.*, "Supercontinuum laser absorption spectroscopy in the mid-infrared range for identification and concentration estimation of a multicomponent atmospheric gas mixture," *Proc. SPIE Remote Sens. Int. Soc. Opt. Photon.*, vol. 8182, 2011, pp. 81820V.

[2] J. T. Walsh, T. J. Flotte, and T. F. Deutsch, "Er:YAG laser ablation of tissue: Effect of pulse duration and tissue type on thermal damage," *Lasers Surgery Med.*, vol. 9, no. 4, pp. 314–326, 1989.

[3] U. Hohenleutner, S. Hohenleutner, W. Bäumler, and M. Landthaler, "Fast and effective skin ablation with an Er:YAG laser: Determination of ablation rates and thermal damage zones," *Lasers Surgery Med.*, vol. 20, no. 3, pp. 242–247, 1997.

[4] W. Chen, X. S. Zhu, R. A. Norwood, F. Song, and N. Peyghambarian, "Numerical investigation on high power mid-infrared supercontinuum fiber lasers pumped at 3 μm," *Opt. Exp.*, vol. 21, no. 24, pp. 29488–29504, 2013.

[5] H. T. Allik *et al.*, "Tunable 7–12-μm optical parametric oscillator using a Cr, Er:YSGG laser to pump CdSe and $ZnGeP_2$ crystals," *Opt. Lett.*, vol. 22, no. 9, pp. 597–599, 1997.

[6] Y. Peng *et al.*, "High-power and widely tunable mid-infrared optical parametric amplification based on PPMgLN," *Opt. Lett.*, vol. 41, no. 1, pp. 49–51, 2016.

[7] Y. Peng *et al.*, "High-power, narrow-bandwidth mid-infrared PPMgLN optical parametric oscillator with a volume Bragg grating," *Opt. Exp.*, vol. 23, no. 24, pp. 30827–30832, 2015.

[8] M. Messner, A. Heinrich, C. Hagen, and K. Unterrainer, "High brightness diode pumped Er:YAG laser system at 2.94 μm with nearly 1 kW peak power," *Proc. SPIE LASE. Int. Soc. Opt. Photon.*, vol. 9726, 2016, pp. 972602.

[9] C. Ziolek *et al.*, "High-repetition-rate, high-average-power, diode-pumped 2.94-μm Er:YAG laser," *Opt. Lett.*, vol. 26, no. 9, pp. 599–601, 2001.

[10] E. Arbabzadah, S. Chard, H. Amrania, C. Phillips, and M. Damzen, "Comparison of a diode pumped Er:YSGG and Er:YAG laser in the bounce geometry at the 3 μm transition," *Opt. Exp.*, vol. 19, no. 27, pp. 25860–25865, 2011.

[11] J. S. Liu, J. J. Liu, and Y. Tang, "Performance of a diode end-pumped Cr, Er:YSGG laser at 2.79 μm," *Laser Phys.*, vol. 18, no. 10, pp. 1124–1127, 2008.

[12] E. A. Arbabzadah, C. C. Phillips, and M. J. Damzen, "Free-running and Q-switched operation of a diode pumped Er:YSGG laser at the 3 μm transition," *Appl. Phys. B*, vol. 111, no. 2, pp. 333–339, 2013.

[13] C. Wyss, W. Luthy, and H. P. Weber, "Modulation and single-spike switching of a diode-pumped Er $^{3+}$: $LiYF_4$ laser at 2.8 μm," *IEEE J. Quantum Electron.*, vol. 34, no. 6, pp. 1041–1045, Jun. 1998.

[14] C. Li *et al.*, "2.8 μm passively Q-switched Er:CaF_2 diode-pumped laser," *Opt. Mater. Exp.*, vol. 6, no. 5, pp. 1570–1575, 2016.

[15] L. Fornasiero, E. Mix, V. Peters, K. Petermann, and G. Huber, "Czochralski growth and laser parameters of RE^{3+}-doped Y_2O_3 and Sc_2O_3," *Ceramics Int.*, vol. 26, pp. 589–592, 2000.

[16] V. Peters *et al.*, "Spectroscopic characterization and diode-pumped laser action at 2.7 μm of Er:Lu_2O_3," in *Proc. CLEO-Europe*, Glasgow, U.K., 1998, p. 379.

[17] T. Li, K. Beil, C. Krankel, and G. Huber, "Efficient high-power continuous wave Er:Lu_2O_3 laser at 2.85 μm," *Opt. Lett.*, vol. 37, no. 13, pp. 2568–2570, 2012.

[18] L. Wang *et al.*, "Diode-pumped high power 2.7 μm Er:Y_2O_3 ceramic laser at room temperature," *Opt. Mater.*, pp. 1–4, 2016.

[19] T. Sanamyan, J. Simmons, and M. Dubinskii, "Efficient cryo-cooled 2.7-μm Er^{3+}:Y_2O_3 ceramic laser with direct diode pumping of the upper laser level," *Laser Phys. Lett.*, vol. 7, no. 8, pp. 569–572, 2010.

[20] T. Sanamyan and Z. Fleischman, "Spectroscopic properties of Er-doped Y_2O_3 ceramic related to mid-IR laser transition," *Proc. SPIE Defense + Security Int. Soc. Opt. Photon.*, vol. 9466, 2015, pp. 946601–946609.

[21] A. Ikesue and Y. L. Aung, "Ceramic laser materials," *Nature Photon.*, vol. 2, no. 12, pp. 721–727, 2008.

[22] L. Wang *et al.*, "Room temperature continuous-wave laser performance of LD pumped Er:Lu_2O_3 and Er:Y_2O_3 ceramic at 2.7 μm," *Opt. Exp.*, vol. 22, no. 16, pp. 19495–19503, 2014.

[23] L. C. Kong *et al.*, "Black phosphorus as broadband saturable absorber for pulsed lasers from 1 μm to 2.7 μm wavelength," *Laser Phys. Lett.*, vol. 13, no. 4, p. 045801, 2016.